

kinesin-I to axonal vesicles (6, 7). If β APP processing to A β s occurs at axonal (or dendritic) blockages and causes kinesin-I release from vesicles and reduction of axonal transport (7), then blockages may lead to local stimulation of β APP processing, which in turn would cause additional vesicle stalling and further local stimulation of β APP processing. This proposed sequence of events would generate an autocatalytic spiral in which processes leading to axonal blockages and A β production become mutually stimulatory. A vicious cycle of axonal blockages and aberrant A β generation also provides a rational explanation for early synaptic loss in AD. Such a mechanism would be critical in AD linked to polymorphisms in KLC1 (37) as well as in sporadic AD, which could potentially be initiated by likely differences in age-dependent declines in axonal transport among humans.

References and Notes

1. S. Yagashita, *Virchows Arch. A Pathol. Anat. Histol.* **378**, 181 (1978).
2. A. D. Cash *et al.*, *Am. J. Pathol.* **162**, 1623 (2003).
3. R. D. Terry, *J. Neuropathol. Exp. Neurol.* **55**, 1023 (1996).
4. E. Masliah *et al.*, *J. Neuropathol. Exp. Neurol.* **52**, 619 (1993).
5. D. J. Selkoe, *Nature* **399**, A23 (1999).
6. A. Kamal, G. B. Stokin, Z. Yang, C. H. Xia, L. S. Goldstein, *Neuron* **28**, 449 (2000).
7. A. Kamal, A. Almenar-Queralt, J. F. LeBlanc, E. A. Roberts, L. S. Goldstein, *Nature* **414**, 643 (2001).
8. H. Papp, M. Pakaski, P. Kasa, *Neurochem. Int.* **41**, 429 (2002).
9. J. G. Sheng, D. L. Price, V. E. Koliatsos, *Exp. Neurol.* **184**, 1053 (2003).
10. P. J. Morin *et al.*, *J. Neurochem.* **61**, 464 (1993).
11. A. E. Roher *et al.*, *Biochemistry* **41**, 11080 (2002).
12. O. Wirths *et al.*, *Brain Pathol.* **12**, 275 (2002).
13. T. Uchihara, H. Kondo, H. Akiyama, K. Ikeda, *Acta Neuropathol.* **90**, 51 (1995).
14. L. Holcomb *et al.*, *Nature Med.* **4**, 97 (1998).
15. U. Muller *et al.*, *Cell* **79**, 755 (1994).
16. J. M. Redwine *et al.*, *Proc. Natl. Acad. Sci. U.S.A.* **100**, 1381 (2003).
17. S. E. Rose *et al.*, *J. Neurol. Neurosurg. Psychiatry* **69**, 528 (2000).
18. S. Gunawardena, L. S. Goldstein, *Neuron* **32**, 389 (2001).
19. T. Kawarabayashi *et al.*, *Neurosci. Lett.* **153**, 73 (1993).
20. D. H. Smith, X. H. Chen, A. Iwata, D. I. Graham, *J. Neurosurg.* **98**, 1072 (2003).
21. Materials and methods are available as supporting material on Science Online.
22. D. R. Borchelt *et al.*, *Neuron* **17**, 1005 (1996).
23. D. R. Borchelt *et al.*, *Neuron* **19**, 939 (1997).
24. P. J. Whitehouse *et al.*, *Science* **215**, 1237 (1982).
25. C. A. Kitt *et al.*, *Science* **226**, 1443 (1984).
26. T. P. Wong, T. Debeir, K. Duff, A. C. Cuello, *J. Neurosci.* **19**, 2706 (1999).
27. D. Hernandez *et al.*, *Neuroreport* **12**, 1377 (2001).
28. P. Davies, A. J. Maloney, *Lancet* **2**, 1403 (1976).
29. H. D. Webster, *J. Cell Biol.* **12**, 361 (1962).
30. R. D. Terry, N. K. Gonatas, M. Weiss, *Am. J. Pathol.* **44**, 269 (1964).
31. L. Torroja, H. Chu, I. Kotovsky, K. White, *Curr. Biol.* **9**, 489 (1999).
32. G. K. Gouras *et al.*, *Am. J. Pathol.* **156**, 15 (2000).
33. E. Masliah *et al.*, *Am. J. Pathol.* **142**, 871 (1993).
34. A. Salehi, J. D. Delcroix, W. C. Mobley, *Trends Neurosci.* **26**, 73 (2003).
35. V. P. Prasher *et al.*, *Ann. Neurol.* **43**, 380 (1998).
36. X. H. Chen *et al.*, *Am. J. Pathol.* **165**, 357 (2004).
37. C. M. Dhaenens *et al.*, *Neurosci. Lett.* **368**, 290 (2004).
38. We thank D. W. Cleveland, F. H. Gage, P. R. Mouton, and R. D. Terry for helpful discussions; M. Yasuda for help with primary hippocampal cultures; M. P. Sundsmo and the UCSD Alzheimer's Disease Research Center (ADRC) for human samples; and the UCSD Cancer Center Digital Imaging Shared Resource for help with imaging. Supported by an Ellison Medical Foundation Senior Scholar Award in Aging Research (L.S.B.G.); NIH grant nos. EY13408, EY12598 (D.S.W.), and P50 AG05131 (A.D.R.C.); a Pew Foundation fellowship (T.L.F.); and a Boehringer-Ingelheim Fonds fellowship (G.B.S.). L.S.B.G. is an Investigator of the Howard Hughes Medical Institute.

Supporting Online Material

www.sciencemag.org/cgi/content/full/307/5713/1282/DC1

Materials and Methods

Figs. S1 to S14

References and Notes

Movies S1 to S5

27 September 2004; accepted 2 December 2004
10.1126/science.1105681

REPORTS

The Use of Transit Timing to Detect Terrestrial-Mass Extrasolar Planets

Matthew J. Holman^{1*} and Norman W. Murray²

Future surveys for transiting extrasolar planets are expected to detect hundreds of jovian-mass planets and tens of terrestrial-mass planets. For many of these newly discovered planets, the intervals between successive transits will be measured with an accuracy of 0.1 to 100 minutes. We show that these timing measurements will allow for the detection of additional planets in the system (not necessarily transiting) by their gravitational interaction with the transiting planet. The transit-time variations depend on the mass of the additional planet, and in some cases terrestrial-mass planets will produce a measurable effect. In systems where two planets are seen to transit, the density of both planets can be determined without radial-velocity observations.

About 130 extrasolar planets (1) have been detected by (i) short-duration brightness anomalies in gravitational microlensing events caused by planets near the lens star (2), (ii) reflex motions of the central star (as revealed

by radial-velocity variations in the stellar spectrum or radio pulse arrival times) (3–6), and (iii) variations in the apparent stellar brightness caused by a planetary transit (passage of the planet in front of the star) (7–11). These approaches provide complementary information. Gravitational microlensing measurements primarily constrain the ratio of planet mass to stellar mass. Radial-velocity measurements lead to estimates of the orbital period, eccentricity, and minimum mass of the planet. With present technology, radial-

velocity surveys can only detect planets with masses greater than about $10 M_{\oplus}$ (orbiting low-mass stars) (12–14). Transit observations provide estimates of the orbital period and planetary radius. Transit surveys, particularly if space based, will be sensitive to planets as small as Mercury for the smallest radius stars observed (15). Barring major improvements in the precision of radial-velocity measurements, the measurement of the mass and radius (and thus the average density) of a terrestrial-sized extrasolar planet would appear to be out of reach.

Here, we point out that variations in the time interval between transits, produced by gravitational interactions with additional planets, allow for the orbital period and mass of the additional planet to be determined from transit observations alone.

The time interval between successive transits of an unperturbed planet is always the same [aside from small corrections due to orbital precession (16) or to the decay of the transiting planet's orbital semimajor axis as a result of tidal interaction with the star (17)]. However, for stellar systems, the presence of a third star orbiting a stellar binary can produce short-term variations, in addition to the more familiar long-term variations, of the period of the binary (18, 19). The same is true for planetary systems. The interval between successive transits of the extrasolar planet HD

¹Harvard-Smithsonian Center for Astrophysics, MS51, 60 Garden Street, Cambridge, MA 02138, USA.

²Canadian Institute for Theoretical Astrophysics, University of Toronto, 60 St. George Street, Toronto, ON M5S 3H8, Canada.

*To whom correspondence should be addressed.
E-mail: mholman@cfa.harvard.edu

209458b would vary by ± 3 s if a second planet (of mass $10^{-4} M_{\odot}$, period 80 days, and eccentricity $e \sim 0.4$) existed in that system (20).

Over the course of their orbits, the transiting planet and a second planet exchange energy and angular momentum as a result of their mutual gravitational interaction. This interaction, greatest at each planetary conjunction, results in short-term oscillations of the semimajor axes and eccentricities of the planets, which in turn alter the interval between successive transits. We illustrate this effect by considering our solar system (Fig. 1). The gravitational perturbations among the planets in the solar system lead to transit-interval variations ranging from tens of seconds for Mercury to thousands of seconds for Mars. The variations for Earth and Venus show oscillations with the 583-day Earth-Venus synodic period. For an exterior transiting planet, the transit interval can be altered by an inner planet's indirect influence on the position of the star, even if the gravitational interaction between the planets is negligible (21).

Next, we investigate the influence of an additional Jupiter-mass planet on the transit interval of HD 209458b. We integrate the heliocentric equations of motion of the hypothetical two-planet system (22). We assume that the two planets are coplanar, have orbits that are perpendicular to the sky plane, and have initially aligned orbital apsides. We include the mutual gravitational interactions of the planets and terms that account for the general relativistic (GR) influence of the central star (23) but neglect the terms for the GR influence of the planetary masses, terms for the oblateness of the star, and terms for the tidal interaction with the star. During the course of each integration, we iteratively solve for the time at which the centers of star and planet reach their minimum projected separation.

Sharp increases in the transit interval occur near the times when the outer planet reaches its periastron (Fig. 2). Hence, the orbital periods of both planets in each of the examples can be determined directly. We chose the period and eccentricity of the hypothetical perturbing planets such that their pericenter distances are roughly the same. As a result, the largest transit-interval variations have comparable magnitude. For clarity, we ignore the light-time effect (21) (due to the varying distance between the star and the observer as the star moves with respect to the center of mass of the star and planets) from the dynamical effects. The magnitude of the light-time effect due to a Jupiter-mass perturber with a 1-AU (astronomical unit) semimajor axis orbiting a solar-mass star is 0.5 s.

Whether the presence of a companion planet can be detected from short-term transit interval variations depends on the difference

between the minimum and maximum transit interval. We consider jovian-mass ($10^{-3} M_{\odot}$) and terrestrial-mass ($3 \times 10^{-6} M_{\odot}$) perturbers. A range of perturber periods is tested, in increments of 0.1 day, starting with the minimum perturber period that ensures that the orbits of the two planets do not initially cross. We follow the same numerical procedure described earlier. During each integration, simulating 10^4 days, we recorded the

times of transit, from which the minimum and maximum intervals between transits were determined. For a given perturber eccentricity, the period variation decreases as the perturber period and semimajor axis increase. Likewise, for a given perturber period, the variation is greater for larger perturber eccentricity. The transit-interval variation is primarily a function of the periastron distance of the perturber, and a com-

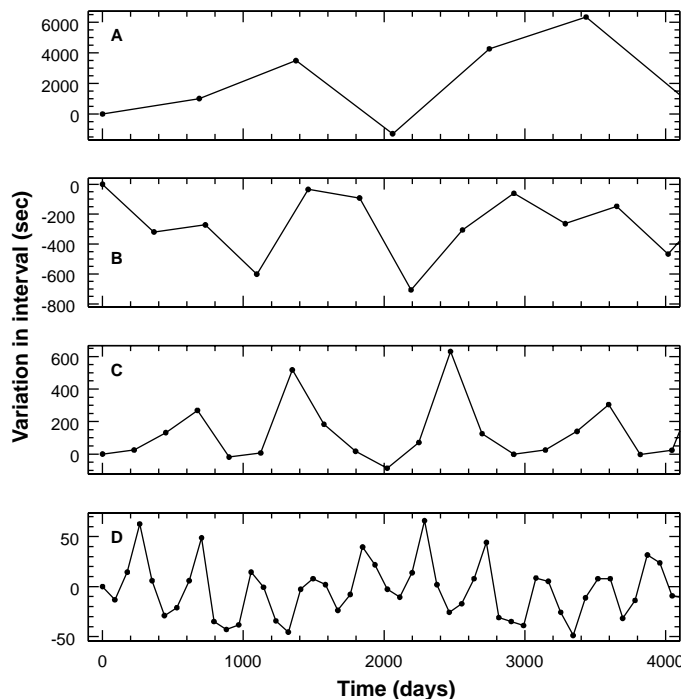


Fig. 1. The variations of the interval between successive transits of terrestrial planets, induced by the other planets in the solar system. (A to D) The variations for Mars, Earth, Venus, and Mercury, respectively. To guide the eye, the solid line connects the times of each transit. The transit intervals result from numerically integrating the equations of motion of the planets in our solar system and calculating the transit times as seen by distant observers located in the present-day orbital planes of the various planets.

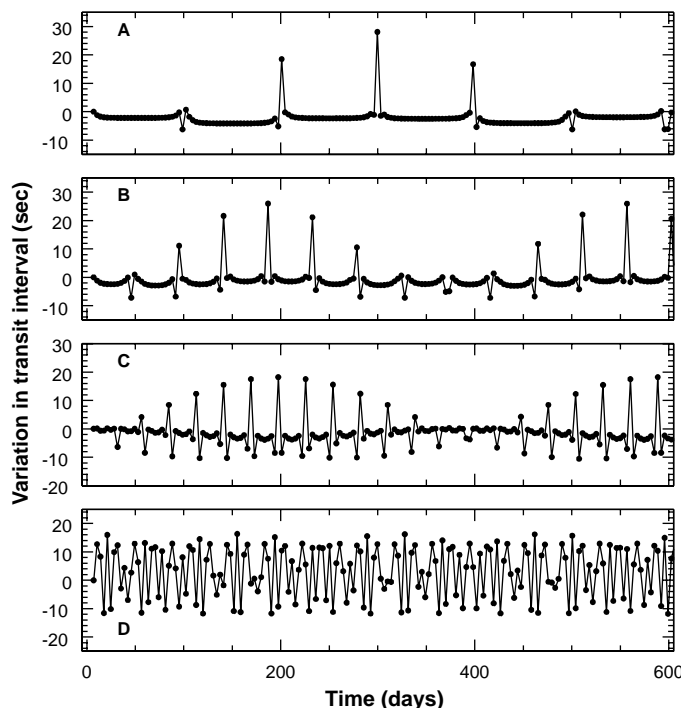


Fig. 2. Transit times of HD 209458b. The numerically determined variation of the interval between successive transit centers of HD 209458b as a function of time, with each panel showing the results for a different set of orbital parameters for a hypothetical second planet with a mass of $M_2 = 10^{-3} M_{\odot}$. In the simulations, HD 209458b has an initial orbital period $P_1 = 3.5248$ days and eccentricity $e_1 = 0.025$. The planets are assumed to be coplanar, with the system viewed edge-on. (A) The results for a perturbing planet with orbital period $P_2 = 99.8$ days and eccentricity $e_2 = 0.7$. (B to D) The results for perturbing planets with orbital periods P_2 of 46.4, 28.0, and 19.2 days and eccentricities e_2 of 0.5, 0.3, and 0.1, respectively. Radial-velocity measurements have ruled out the presence of such planets in the actual HD 209458b system (20).

parison of our different perturber simulations (Figs. 3 and 4) confirms that the magnitude of the effect is proportional to the perturber mass. For time spans shorter than the orbital period of the transiting planet, the magnitude of the effect is independent of the mass of the transiting planet (a result that follows from the equivalence of inertial and gravitational mass).

We estimate the variation in transit intervals for an inner transiting planet by integration of Lagrange's equations of planetary motion (24). Given a transiting planet with semimajor axis a_1 and period P_1 , and a perturbing planet with semimajor axis a_2 (where $a_2 > a_1$), period P_2 , and mass M_2 , we find

$$\Delta t \approx \frac{45\pi}{16} \left(\frac{M_2}{M_*}\right) P_1 \alpha_e^3 (1 - \sqrt{2}\alpha_e^{3/2})^{-2} \quad (1)$$

where Δt is the magnitude of the typical variation of the interval between successive transit

and $\alpha_e = \{(a_1)/[a_2(1 - e_2)]\}$. Equation 1 was derived by assuming that the perturber follows a parabolic orbit with a periastron distance of $a_2(1 - e_2)$. It underestimates the actual variation in transit period for small period ratios and best matches the numerical results for $e_2 \geq 0.3$. The transit-interval variations increase with P_1 when the period ratio of the two planets is held fixed. Thus, for a fixed timing accuracy, the detection of companions is easier for systems where the transiting planet is farther from the star. For a given perturbing planet mass, the timing variations are also larger for planets orbiting less massive stars.

The eccentricity of the outer planet can be estimated from the relative magnitudes of the variations $\Delta t_{\max}/\Delta t_{\min}$. If the period of the perturbing planet is much greater than that of the transiting planet, the final factor of Eq. 1 can be ignored. The resulting equa-

tion can be rearranged to provide an estimate of the mass of the perturbing planet

$$M_2 \approx \frac{16}{45\pi} M_* \frac{\Delta t_{\max}}{P_1} \left(\frac{P_2}{P_1}\right)^2 (1 - e_2)^3 \quad (2)$$

given an estimate of e_2 .

Large excursions in transit-interval variation (Figs. 3 and 4) occur near small integer ratios of the orbital periods of the two planets, the locations of mean-motion resonances between the planets. In and near mean-motion resonances, the planets undergo larger oscillations of semimajor axis and eccentricity (24). The width in semimajor axis of each resonance region is proportional to $a_2(M_*/M_2)^{1/2}$ and grows rapidly with increasing eccentricity (24). The ranges of perturber periods (Figs. 3 and 4) in which the transit-interval variations are irregular correspond to dynamical chaos that results from the overlap of adjacent mean-motion resonances (25). We have excluded the ranges of perturber period in which this chaos results in short-term dynamical instability because such planetary configurations are unlikely to be found.

The two planets of the GJ 876 system provide an excellent example of a 2:1 mean-motion resonance in an extrasolar planetary system. Because of the resonant gravitational interaction between the two planets, the orbital periods of the inner and outer planet vary from 30.1 days to 31.1 days and from 60.0 days to 59.1 days, respectively, over a libration period of 550 days (26). Although careful photometric monitoring has excluded the possibility of transits of the inner planet of the GJ 876 system (27), such transit-interval variations would be seen if the inner planet transited.

In some cases, the libration period of a resonant system can be much longer than the interval of observation. Thus, the transit-interval variations due to the resonance cannot be easily discerned, even if the amplitude of the variation is large. GJ 876's short libration period, P_{lib} , results from the combination of its low-mass star ($M_* = 0.4 M_\odot$) and massive planets ($M_1 = 2 M_{\text{Jup}}$, $M_2 = 4 M_{\text{Jup}}$), because $P_{\text{lib}} \propto P_1(M_*/M_2)^{1/2}$ (26, 24) (and depends on the order of the resonance). The 10^4 day integrations used for Figs. 3 and 4 are long enough to sample a full libration period for the low-order resonances. A corresponding system with a solar-mass star, a 1-year orbital period for the inner planet, and Jupiter-mass planets in the 2:1 resonance would have a libration period of ~ 50 years. For Earth-mass planets, the libration period would be nearly 1000 years. These long-term effects would not be observable. However, the smaller transit-interval variations that occur on the time scale of the orbital periods of the two planets could be observed.

The feasibility of using this technique to detect additional planets in transiting systems

Fig. 3. Variations in the interval between successive transits of a planet with orbital period $P_1 = 3$ days, eccentricity $e_1 = 0.01$, and mass $M_1 = 10^{-3} M_\odot$, induced by a second planet with mass $M_2 = 10^{-3} M_\odot$. The planets are assumed to be coplanar. The black lines show the maximum transit-time variation as a function of orbital period (or semimajor axis) and eccentricity of the outer planet. The star has mass $M_* = M_\odot$. The red dashed lines show the estimate given by Eq. 1.

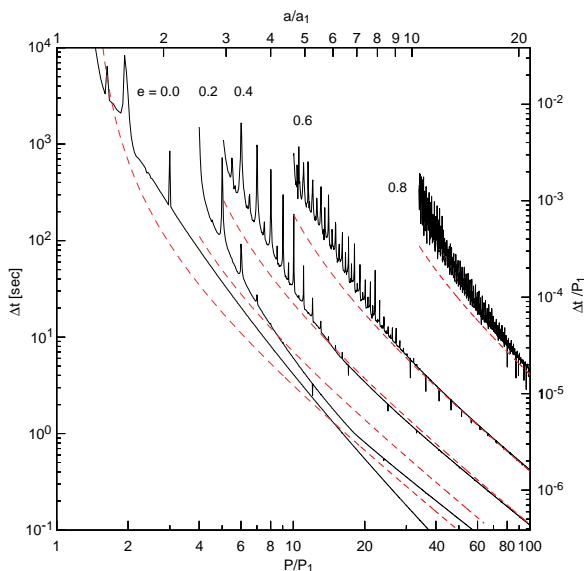
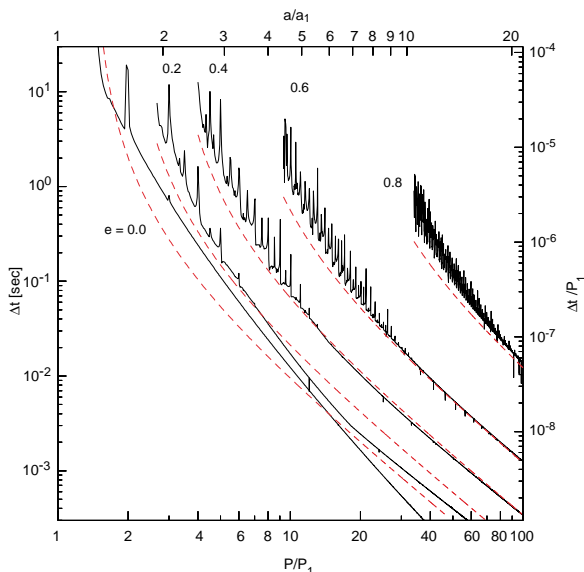


Fig. 4. Variations in the interval between successive transits of a planet with orbital period $P_1 = 3$ days, eccentricity $e_1 = 0.01$, and mass $M_1 = 10^{-3} M_\odot$, induced by a second planet with mass $M_2 = 3 \times 10^{-6} M_\odot$. The planets are assumed to be coplanar. The black lines show the maximum transit-time variation as a function of orbital period (or semimajor axis) and eccentricity of the outer planet. The star has mass $M_* = M_\odot$. The red dashed lines show the estimate given by Eq. 1.



depends on the physical and orbital properties of the multiple planet systems, the accuracy with which the times of transit can be measured, and the time span of the observations. Our expectations for systems with multiple Neptune-mass to Jupiter-mass planets are guided by recent discoveries, as well as by the giant planets in our solar system. Fourteen of 117 systems are known to have two or more planets. These have period ratios ranging from 2 to 150, and three are known or thought to be in mean-motion resonances. In the solar system, neighboring giant planets have period ratios of two to three. The eccentricities of the planets in the solar system are small, but in many of the extrasolar planetary systems the eccentricities are large, ranging up to $e = 0.9$.

Both the theory of terrestrial-planet formation and available observations suggest that the typical terrestrial-planet system will have a configuration that results in variations in the transit interval of hundreds of seconds over time spans of months to years. Because the escape velocity from the surface of a terrestrial planet is smaller than the escape velocity from a solar-mass star at ~ 1 AU, all the solid material in the region from a few tenths to one or two AU must either accrete into planets or fall onto the star. The resulting planets are as closely spaced as dynamical stability permits (28, 29). As observed in the solar system and in the pulsar planet system, the period ratios are of order two.

Assuming that the observations during the ingress and egress of a transit are well sampled, the error σ_{t_c} (due to photon statistics alone) associated with the measured time of the center of a transit of duration t_T is given by

$$\frac{\sigma_{t_c}}{t_T} \sim (\Gamma t_T)^{-1/2} \rho^{-3/2} \quad (3)$$

where Γ is the photon count rate of the star and $\rho = R_p/R_*$ is the ratio of the planet radius to the stellar radius. Kepler (15), a NASA Discovery mission, will monitor 100,000 A-M dwarf stars brighter than apparent magnitude $V = 14$, looking for transits of terrestrial-sized planets in the habitable zone (30). The smaller mission, COROT, will monitor 12,000 dwarf stars with apparent magnitudes of $V = 11$ to $V = 16$, also searching for terrestrial-mass planets (31). For Kepler, with its 0.95-m-diameter aperture, $\Gamma = 7.8 \times 10^8 10^{-0.4(V-12)} \text{ h}^{-1}$, for a star of apparent magnitude V . For a Jupiter-sized planet in a 1-year orbit about a solar-mass star with $V = 12$, we find $\sigma_{t_c} \sim 20$ s ($\rho \sim 0.1$, $t_T \sim 13$ h). For a terrestrial-sized planet, $\sigma_{t_c} \sim 500$ s ($\rho \sim 0.01$). These accuracies suggest that the transit-period variations due to the gravitational influence on each other of Earth-mass planets with small period ratios can be detected by Kepler. The observing cadence for Kepler will be limited by the rate at which the data are transmitted to Earth. This will nominally be 15 min but will be reduced to 1 min for likely transit candidates.

For brighter stars observed with large-aperture ground-based telescopes, the presence of more distant additional planets can be detected. For example, observing a $V = 9$ star with a 6.5-m-aperture telescope, $\sigma_{t_c} \sim 0.2$ s. For such a star, the photon noise exceeds the errors due to atmospheric scintillation after ~ 30 s of accumulated integration (32). Also, microvariability at the level of 10 to 50 parts per million is expected from p-mode oscillations such as those seen in the sun, with characteristic periods of 300 s. This noise source is competitive with shot noise in 8-m-class telescopes for $V = 14$ stars.

One would like to measure the density of a transiting planet to determine whether it is a rocky terrestrial planet such as Earth, an ice/water giant such as Neptune, or a gas giant planet such as Jupiter. Unfortunately, when a transiting planet is perturbed by a nontransiting planet, photometry yields the radius of the transiting planet but not its mass, whereas the transit times yield the mass of the perturbing planet but not its radius. Thus, neither planet's density can be determined.

In cases in which two or more planets transit their star, the masses and radii of each planet can be estimated, allowing density determinations for all. For such systems, radial-velocity observations will not be necessary to determine their masses and densities. Many of the target stars in future surveys will be too faint to allow for radial-velocity detections of terrestrial-mass planets, even with technical improvements to the accuracy of such measurements. Thus, the transit-timing technique may be the only means to estimate the mass and density of terrestrial-mass planets. If one sees transits of one planet in a multiple-planet system, what is the probability of seeing transits of a second planet? Assuming that the orbits of the two planets are coplanar, the probability that the second planet also transits is a_1/a_2 if $a_2 > a_1$ (if $a_2 < a_1$, transits of the second planet are assured in the case of coplanar orbits). If the orbits of the two planets are mutually inclined and one planet transits the center of the star, the probability that the second planet also transits is

$$P_{t_2} = \frac{2}{\pi} \arcsin\left(\frac{R_*}{a_2 \sin i'}\right) \quad (4)$$

where i' is the mutual inclination between the orbits of the two planets rather than the sky-plane inclination. This assumes $\sin i' > R_*/a_2$; otherwise, transits of the second planet are certain. For a solar-radius star, a mutual inclination of a few degrees, and a semimajor axis $a_2 \sim 1$ AU, the probability is roughly 10%. Thus, such double-transiting systems are likely to be found.

The Kepler team plans to search for transits with a consistent period, depth, and duration (15). We caution that any detection algorithm that looks for evidence of periodic transits in

the photometry must allow for variations in the transit period due to the perturbations from unseen planets. An overly restrictive test for periodicity might reject some of the most interesting and informative planetary systems. The GJ 876 system discussed above, an extreme case, might be rejected as only quasiperiodic.

We also caution that experiments looking for gradual transit-period variations due to slow secular trends must allow for the possibility of substantial short-term variations in the transit period. Transit-period variations due to orbital precession (16) or to tidal interaction with a star (17) require many years to elapse before they can be detected; without careful monitoring in the interim to determine the short-term variations, the results of such experiments could easily be misinterpreted.

References and Notes

1. J. Schneider (2004); www.obspm.fr/encycl/catalog.html.
2. I. A. Bond *et al.*, *Astrophys. J.* **606**, L155 (2004).
3. A. Woloszczan, D. A. Frail, *Nature* **355**, 145 (1992).
4. D. C. Backer, R. S. Foster, S. Sallmen, *Nature* **365**, 817 (1993).
5. M. Mayor, D. Queloz, *Nature* **378**, 355 (1995).
6. G. W. Marcy, R. P. Butler, *Astrophys. J.* **464**, L147 (1996).
7. D. Charbonneau, T. M. Brown, D. W. Latham, M. Mayor, *Astrophys. J.* **529**, L45 (2000).
8. G. W. Henry, G. W. Marcy, R. P. Butler, S. S. Vogt, *Astrophys. J.* **529**, L41 (2000).
9. A. Udalski *et al.*, *Acta Astron.* **52**, 1 (2002).
10. A. Udalski *et al.*, *Acta Astron.* **52**, 115 (2002).
11. A. Udalski *et al.*, *Acta Astron.* **53**, 133 (2003).
12. B. E. McArthur *et al.*, *Astrophys. J.* **614**, L81 (2004).
13. P. Butler *et al.*, *ArXiv Astrophysics e-prints*, astro-ph/0408587 (2004).
14. R. Narayan, A. Cumming, D. N. C. Lin, *ArXiv Astrophysics e-prints*, astro-ph/0409766 (2004).
15. W. J. Borucki *et al.*, in *Future EUV/UV and Visible Space Astrophysics Missions and Instrumentation*, J. C. Blades, O. H. W. Siegmund, Eds. Proceedings of the SPIE, Vol. 4854, pp. 129–140 (2003).
16. J. Miralda-Escudé, *Astrophys. J.* **564**, 1019 (2002).
17. D. D. Sasselov, *Astrophys. J.* **596**, 1327 (2003).
18. E. W. Brown, *Mon. Not. R. Astron. Soc.* **97**, 62 (1936).
19. S. Soderhjelm, *Astron. Astroph.* **42**, 229 (1975).
20. P. Bodenheimer, G. Laughlin, D. N. C. Lin, *Astrophys. J.* **592**, 555 (2003).
21. E. Agol, J. Steffen, R. Sari, W. Clarkson, *ArXiv Astrophysics e-prints*, astro-ph/0412032 (2004).
22. J. Stoer, R. Bulirsch, *Introduction to Numerical Analysis* (Springer-Verlag, New York, 1980).
23. T. R. Quinn, S. Tremaine, M. Duncan, *Astron. J.* **101**, 2287 (1991).
24. C. D. Murray, S. F. Dermott, *Solar System Dynamics* (Cambridge Univ. Press, Cambridge, 1999).
25. J. Wisdom, *Astron. J.* **85**, 1122 (1980).
26. G. Laughlin, J. E. Chambers, *Astrophys. J.* **551**, L109 (2001).
27. G. Laughlin (2004); www.transitsearch.org.
28. J. E. Chambers, G. W. Wetherill, *Icarus* **136**, 304 (1998).
29. E. Kokubo, S. Ida, *Icarus* **131**, 171 (1998).
30. J. F. Kasting, D. P. Whitmire, R. T. Reynolds, *Icarus* **101**, 108 (1993).
31. C. Catala *et al.*, *Astronomical Society of the Pacific Conference Series* **76**, 426 (1995).
32. R. L. Gilliland *et al.*, *Astron. J.* **106**, 2441 (1993).
33. This work was supported in part by NSF grant PHY99-07949 and by NASA grant NAG5-9678. This research was supported by the Natural Sciences and Engineering Research Council of Canada and by the Canada Research Chair program. N.W.M. is a Canada Research Chair. We are grateful to the Kavli Institute for Theoretical Physics, where much of this investigation was carried out. We thank S. Gaudi and J. Winn for helpful discussions and careful reviews of the manuscript.

23 November 2004; accepted 21 January 2005
10.1126/science.1107822